

Equilibrium reconstruction on W7-X stellarator using Function Parametrization

A.Sengupta¹, J.Geiger², P.J.McCarthy¹

¹*Dept. of Physics, University College Cork, Association EURATOM-DCU, Cork, Ireland*

²*Max-Planck-Institut für Plasmaphysik, Euratom Association, Greifswald, Germany*

1. Introduction

W7-X [1] is a fully optimized stellarator of the Helias type, with a five-fold toroidal symmetry (i.e., five toroidal periods), under construction at the Max-Planck Institut für Plasmaphysik (IPP), Greifswald, Germany. With an average major radius of 5.5 m and an average minor radius of 55 cm, the aspect ratio of W7-X is ~ 10 .

After the analysis, using Function Parametrization (FP), of the vacuum configurations of W7-X with magnetic islands [2], the analysis at finite- β was started last year and reported [3,4]. The results of [2] were encouraging enough to use FP again. Magnetic configurations in presence of plasma pressure are important because of significant changes to the vacuum flux surface topology at finite- β . W7-X is fully optimized in the sense that the plasma influence on the magnetic configuration has been strongly reduced by the minimization of bootstrap and Pfirsch-Schlüter currents. This provides good MHD stability properties up to $\langle \beta \rangle = 5\%$. Additionally, good fast particle confinement at finite- β has been included in the configurations.

For the present study we neglected the presence of magnetic islands in the equilibrium configurations. Islands in finite- β conditions can be simulated only with codes like HINT [5] or PIES [6] which are computationally too demanding to be used for statistical analyses. Furthermore, the external coils of W7-X were assumed to be accurately positioned, and error fields arising from, e.g., coil misalignments, were not included in our statistical model.

2. Database generation and choice of predictors for FP model

The database generation details, along with the criteria for the choice of the final set of (~ 8000) observations in the database, were described in [3,4] and so will not be repeated here, but for the benefit of the readers we are quoting again the parametrization of the plasma pressure $p(s)$ and the toroidal current $I(s)$ profiles:

$$p(s) = \sum_{i=1}^n a_i b_i(s) \quad ; \quad I(s) = \sum_{i=1}^n c_i d_i(s)$$

where $b_i(s)$ and $d_i(s)$ are polynomials of degree i in the normalized toroidal flux s and represent the i th moment of the pressure and the toroidal current distribution, and $n = 4$.

However, we will discuss the major difference of this study with [3,4], namely, the choice of predictors for the FP model. For the coil currents, the chosen predictors were the (6) current ratios, while the plasma size a_{eff} formed a predictor itself. For the plasma pressure and toroidal current data, the independently-generated coefficients a_i and c_i of the $p(s)$ and $I(s)$ representation were used as predictors in [3,4]. However, their inclusion involves the problem of having to derive them from (noisy) experimental pressure and toroidal current profile data. Since the coefficients of the higher order moments become increasingly sensitive to noise, the

quality of plasma parameter recovery rapidly worsens with increase of noise level. That is why we chose the more robust approach of a Principal Component Analysis (PCA) of the profile data, and the significant principal components (PC's), meaning those PC's with significant eigenvalues or variance, were the inputs to our model. The actual PCA was carried out on the noiseless profile data, and the corresponding eigenvectors of the significant PC's were stored. The noisy PC's were then calculated by a linear combination of the stored (noiseless) eigenvectors with the noisy profile data. The advantages of this method are the following:

(i) the PC's do not show strong sensitivity to noise when derived from noisy profile data;

(ii) a PCA of the profile data can be carried out for any functional form of the profile.

The PCA of the profile data showed that the first four PC's accounted for the entire 100% of the radial variation for both $p(s)$ and $I(s)$. This completed the set of 15 predictors for our regression. The PCA result was expected, because the simulated profile data were generated from the parametrizations of $p(s)$ and $I(s)$, where the profile variables vary linearly with the coefficients $a_1 - a_4$ and $c_1 - c_4$, respectively.

The basic plasma parameters chosen for the recovery were the profiles (as functions of an effective flux surface radius r_{eff}) of t and the Fourier coefficients of the magnetic field strength (B_{mn}), the geometry (R_{mn}, Z_{mn}) and the periodic renormalization function (λ_{mn}), where m and n are, respectively, the poloidal and the toroidal Fourier mode number. However, instead of the conventional method of polynomials in r_{eff} , which proved to be too impractical to be used with 15 predictors, we chose a modified method to recover the plasma profile parameters. This method involved a PCA of the profile function, valued at 21 radial points, with the significant PC's

forming the response variables for the regression model, as described in [3,4]. The model was then tested on a separate test dataset. The model coefficients, determined from the "training" dataset (~ 5000 observations), were combined with the (quadratic or cubic) combinations of the predictors in the test dataset (~ 2400 observations) to recover the radial moments of the plasma profile variables. The recovered moments, or PC's, were then linearly combined with the radial eigenvectors to get the recovered plasma parameters at the 21 radial points.

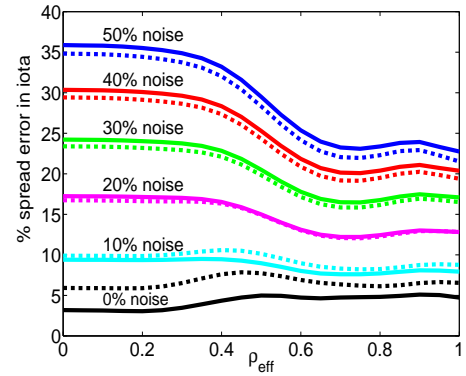


Figure 1: Error profiles of iota recovery for different noise levels. Solid line: c-FP model; Dashed line: q-FP model.

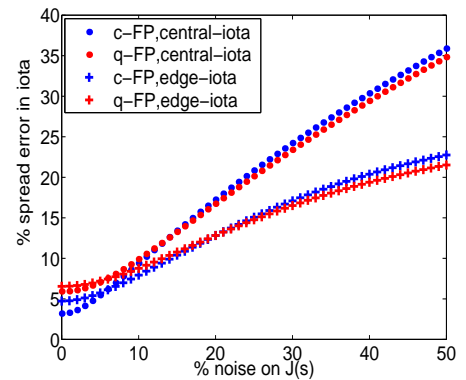


Figure 2: Central- and edge-iota recovery error as a function of measurement noise, with noise on J -profile quoted on abscissa.

3. Adding measurement noise

For the recovery of the parameters of the plasma magnetic configuration, the following noise scheme was used to perturb the “measurements”. For the coil currents, we chose to add a small error to the currents, even though the estimated uncertainty is very small. The error was quantified as 0.1% of the database rms values of the currents, or 11 amps for the modular field coils and 7 amps for the planar coils. This level of noise in the coil currents was kept constant throughout the “experiment”. For the toroidal plasma current, the current density profile, $J(s)$, is usually the known quantity (from transport analysis) with its uncertainties, so noise was added to $J(s)$ obtained by finite differencing the database $I(s)$. The added noise was $x\%$ of the database rms values of $J(s)$ as a function of the flux coordinate s . The relative noise x was uniform along the profile. The values of x were from 1% up to 50%. The noisy $\tilde{J}(s)$ was summed to generate a noisy $\tilde{I}(s)$ profile. The edge value $\tilde{I}(s = 1)$, however, was replaced by that corresponding to the known, estimated noise level (0.1% random noise and 0.5% systematic noise, on the maximum expected current of 50 kA) for its independent measurement.

For the pressure data a basically similar scheme was followed, the noise being $y\%$ of the database (flux-dependent) mean value of the pressure. However, the value of y ranged from 0 only up to 20% as it is usually anticipated that the plasma pressure is more accurately determined than the current density. The noise scan for a_{eff} was limited to 10% of the database mean value.

4. Recovery results

Fig 1 shows the error profiles for t -recovery using c-FP (solid lines) and q-FP (dashed lines) for various values of measurement noise. Plotted along the abscissa is ρ_{eff} , which is the normalized r_{eff} . The c-FP recovery errors are significantly smaller for low levels of noise, but this superiority of c-FP weakens as the noise level is ramped up. For noise $\geq 20\%$, q-FP errors are smaller, though only very slightly, than c-FP errors. The two sets of plots in fig 2 show the percentage error for the recovery of central- and edge- t as a function of percentage measurement error, the abscissa showing the noise scan on $J(s)$. The curves plotted in dots are for the recovery of central- t . We again find that for low levels of measurement noise c-FP is clearly the better model, but its difference with q-FP decreases as the noise increases. At 13%, the blue and red dots coincide, before the q-FP curve goes below the c-FP. The curves plotted in ‘+’ describe the results for edge- t recovery. One difference with central- t recovery is that the blue and the red curves now meet at 20% of measurement noise,

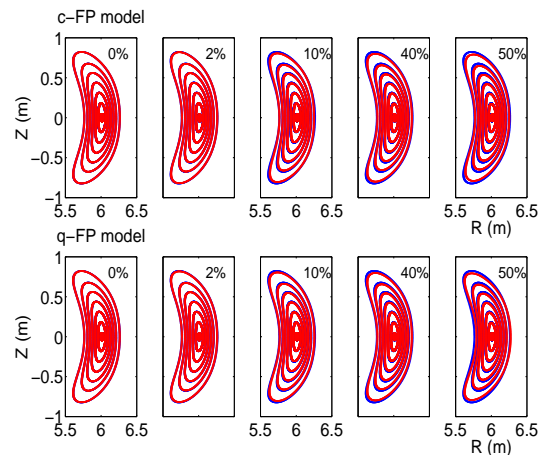


Figure 3: Flux surface recovery in the bean-shaped plane. Quoted are percentage noise on $J(s)$. Blue: VMEC surfaces; Red: FP-recovered surfaces.

the other being the larger edge- t error compared to the central- t error for exact measurements, and the larger central- t error compared to the edge- t error at high levels of measurement noise. Fig 3 shows the bean-shaped cross section of the W7-X flux surfaces on the toroidal angle $\phi=0$ plane, for one randomly chosen case in the test dataset. The VMEC flux surfaces are shown in blue, while the FP-recovered surfaces are in red. The upper panel shows the c-FP recovery, while the lower one corresponds to q-FP. The recovered flux surfaces compare well with the observed ones up to 10% noise. The positive aspect of the flux surface recovery is the fitting of the indentation. Above 10% measurement noise, the recovered surfaces do deviate from the observed surfaces, but the q-FP seems to show a smaller deviation. Fig 4 shows the comparison of the VMEC flux surfaces with the FP-recovered surfaces in the triangular plane for $\phi=36$, for the same observation as plotted in fig 3. The tip of the triangular cross section on the outboard side shows a greater sensitivity to noise, as the deviations start from there at $\leq 10\%$ noise.

5. Conclusions

Equilibrium reconstruction of W7-X magnetic configuration at finite- β using essentially non-magnetic measurements showed excellent recovery accuracy at low levels of measurement noise, usually up to around 10% on $J(s)$, using a cubic polynomial model. This supported earlier results on vacuum analysis. The results obtained with exact inputs would be very useful in a rapid generation of a large database, thereby avoiding the use of time-consuming equilibrium codes. With increase of measurement noise the initially superior performance of the cubic model weakened, and finally reversed (though only slightly in general). In the worst case scenario of the chosen noise limits, that corresponded to 50% of $J(s)$ -profile noise, 20% of pressure profile noise and 10% noise in a_{eff} , the two models performed similarly. However, c-FP should still be the recommended model due to its overall reliability.

References

- [1] Beidler C. et al 1990 *Fusion Technol.* **17** 148
- [2] Sengupta A., Mc Carthy P.J., Geiger J., Werner A. 2004 *Nucl. Fusion* **44** 1176
- [3] Sengupta A., Geiger J., Mc Carthy P.J. *32nd European Physical Society conference on Plasma Physics, Tarragona, Spain (June 27 - July 1, 2005)* P2.047
- [4] Mc Carthy P.J., Sengupta A., Geiger J., Werner A. *15th International Stellarator Workshop, Madrid, Spain (October 3 - 7, 2005)* P2-09
- [5] Harafuji K., Hayashi T. and Sato T. 1989 *J. Comp. Phys.* **81** 169
- [6] Reiman A.H. and Greenside H.S. 1986 *Comput. Phys. Commun.* **43** 157

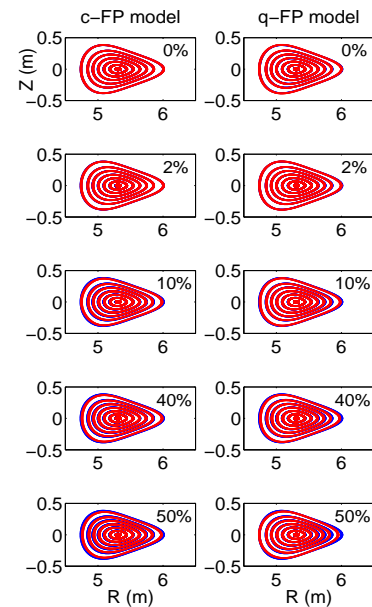


Figure 4: Flux surface recovery in the triangular plane. Quoted are percentage noise on $J(s)$. Blue: VMEC surfaces; Red: FP-recovered surfaces.